Universality in four-dimensional random-field magnets

Fytas, N. and Theodorakis, P.E.

Original citation & hyperlink:
Fytas, N. and Theodorakis, P.E. (2015) Universality in four-dimensional random-field magnets. European Physical Journal B, volume 88 : 205
http://dx.doi.org/10.1140/epjb/e2015-60362-4

DOI 10.1140/epjb/e2015-60362-4
ISSN 1434-6028
ESSN 1434-6036

Publisher: Springer

The final publication is available at Springer via http://dx.doi.org/10.1140/epjb/e2015-60362-4

EPJ manuscript No.
(will be inserted by the editor)

Universality in four-dimensional random-field magnets

Nikolaos G. Fytas[1a] and Panagiotis E. Theodorakis[2]

[1] Applied Mathematics Research Centre, Coventry University, Coventry, CV1 5FB, United Kingdom
[2] Department of Chemical Engineering, Imperial College London, London SW7 2AZ, United Kingdom

Received: date / Revised version: date

Abstract. We investigate the universality aspects of the four-dimensional random-field Ising model (RFIM) using numerical simulations at zero temperature. We consider two different, in terms of the field distribution, versions of the model, namely a Gaussian RFIM and an equal-weight trimodal RFIM. By implementing a computational approach that maps the ground-state of the system to the maximum-flow optimization problem of a network, we employ the most up-to-date version of the push-relabel algorithm and simulate large ensembles of disorder realizations of both models for a broad range of random-field values and system sizes. Using as finite-size measures the sample-to-sample fluctuations of the order parameter of the system, we propose, for both types of distributions, estimates of the critical field h_c and the critical exponent ν of the correlation length, the latter suggesting that the two models in four dimensions share the same universality class.

PACS. PACS. 05.50+q Lattice theory and statistics (Ising, Potts. etc.) – 64.60.De Statistical mechanics of model systems – 75.10.Nr Spin-glass and other random models

1 Introduction

The RFIM is one of the archetypal disordered systems [1–3], extensively studied due to its theoretical interest, as well as its close connection to experiments in hard [4, 5] and soft condensed matter systems [6]. Its beauty is that the mixture of random fields and the standard Ising model creates rich physics and leaves many still unanswered problems. The Hamiltonian describing the model is

$$\mathcal{H} = -J \sum_{<i,j>} \sigma_i \sigma_j - \sum_i h_i \sigma_i, \qquad (1)$$

where $\sigma_i = \pm 1$ are Ising spins, $J > 0$ is the nearest-neighbor's ferromagnetic interaction, and h_i are independent quenched random fields.

The existence of an ordered ferromagnetic phase for the RFIM, at low temperature and weak disorder, followed from the seminal discussion of Imry and Ma [1], when the space dimension is $d > 2$ [7–11]. This has provided us with a general qualitative agreement on the sketch of the phase boundary, separating the ordered ferromagnetic phase from the high-temperature paramagnetic one. The phase-diagram line separates the two phases of the model and intersects the randomness axis at the critical value of the disorder strength h_c, as shown in Figure 1. For low temperatures and small randomness, the ferromagnetic couplings dominate, hence the system exhibits a long-range order. For higher temperatures, where the entropy dominates, or for higher random fields, where the spins are predominately aligned parallel to its local random fields, the system is paramagnetic. Such qualitative sketching has been commonly used for the RFIM [12–14] and closed form quantitative expressions are also known from the early mean-field calculations [15] and more recently from extensive Monte Carlo simulations [16].

The criteria for determining the low-temperature phase transition and its dependence on the form of the field distribution have been discussed throughout the years [15, 17, 18]. Although the view that the phase transition of the RFIM is nowadays considered to be of second order [19–24], the extremely small value of the exponent β casts some doubt on the interpretation of numerical and experimental results. Moreover, a rather strong debate with regards to the role of disorder, i.e., the dependence, or not, of the critical exponents on the particular choice of the distribution for the random fields and the value of the disorder strength, analogously to the mean-field theory predictions [15], was only recently put on a different basis [25]. Currently, even the well-known correspondence among the RFIM and its experimental analogue, the diluted antiferromagnet in a field, has been severely questioned by extensive simulations performed on both models at positive- and zero-temperature [26]. In any case, the whole issue of the model's critical behavior is still under intense investigation [19–37].

Already from the work of reference [38], the importance of the form of the distribution function in the deter-

[a] e-mail:nikolaos.fytas@coventry.ac.uk

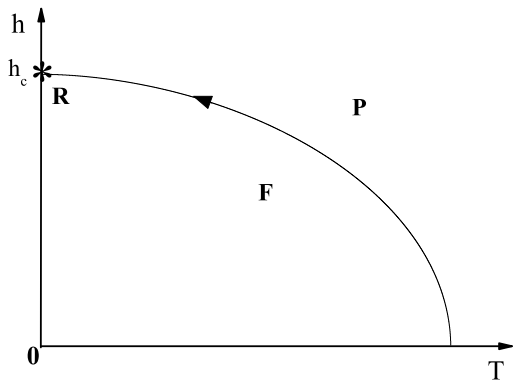

Fig. 1. Schematic phase diagram and renormalization-group flow of the RFIM (for simplicity we have set $J = 1$). The solid line separates the ferromagnetic (**F**) and paramagnetic (**P**) phases. The black arrow shows the flow to the random fixed point (**R**) at $T = 0$ and $h = h_c$, as marked by an asterisk.

mination of the critical properties of the RFIM has been emphasized. In fact, different results have been proposed for different field distributions, like the existence of a tricritical point at the strong disorder regime of the system, present only in the bimodal case [15,38]. Following the results of Houghton et al. [38], Mattis [39] reexamined the RFIM introducing a new type of a trimodal distribution

$$\mathcal{P}^{(\mathrm{trimodal})}(h_i) = p\delta(h_i) + \left(\frac{1-p}{2}\right)[\delta(h_i - h) + \delta(h_i + h)], \tag{2}$$

where h defines the disorder (field) strength and $p \in (0, 1)$. Clearly, for $p = 1$ one switches to the pure Ising model, whereas for $p = 0$ the well-known bimodal distribution is recovered. In general terms, the trimodal distribution (2) allows a physical interpretation as a diluted bimodal distribution, in which a fraction p of the spins are not exposed to the external field. Thus, it mimics the salient feature of the Gaussian distribution

$$\mathcal{P}^{(\mathrm{Gaussian})}(h_i) = \frac{1}{\sqrt{2\pi h^2}} \exp\left(-\frac{h_i^2}{2h^2}\right), \tag{3}$$

for which a significant fraction of the spins are in weak external fields. Mattis suggested that for a particular case, $p = 1/3$, equation (2) may be considered to a good approximation as the Gaussian distribution [39]. This in turn indicated that the two models should be in the same universality class. Further studies along these lines, using mean-field and renormalization-group approaches, provided contradicting evidence for the critical aspects of the $p = 1/3$ model and also proposed several approximations of its phase diagram for a range of values of p [40–42]. Only very recently accurate numerical data at zero temperature have been presented at $d = 3$, indicating that the original suggestion of Mattis is most probably correct [43].

The scope of the present work is to test whether the prediction of reference [39] is valid at higher dimensions, however still below the upper critical one ($d_u = 6$), for which universality has been questioned [29]. In particular, we choose to study the two versions of the RFIM at $d = 4$, suitably away from d_u, where the effect of logarithmic corrections may obscure the scaling analysis [45]. Additionally, for the Gaussian model our results can be directly compared to those of some previous numerical studies [46,47]. Our attempt benefits from the existence of robust graph-theoretical computational methods at zero temperature ($T = 0$) that allow us to simulate large system sizes and disorder ensembles in moderate computational times and is based upon a scaling approach defined with the help of the sample-to-sample fluctuations of the order parameter of the system.

The rest of the paper is organized as follows: In the next Section we describe briefly the numerical approach and provide all the necessary details of our implementation. The relevant finite-size scaling analysis is presented in Section 3. We synopsize our findings in Section 4.

2 Numerical scheme

As already discussed extensively in the literature [48], the RFIM captures essential features of models in statistical physics that are controlled by disorder. Such systems show complex energy landscapes due to the presence of large barriers that separate several meta-stable states. When such models are studied using simulations mimicking the local dynamics of physical processes, it takes an extremely long time to encounter the exact ground state. However, there are cases where efficient methods for finding the ground state can be utilized and, fortunately, the RFIM is one such case. These methods escape from the typical direct physical representation of the system, in a way that extra degrees of freedom are introduced and an expanded problem is finally solved. By expanding the configuration space and choosing proper dynamics, the algorithm practically avoids the need of overcoming large barriers that exist in the original physical configuration space. An attractor state in the expended space is found in time polynomial in the size of the system and when the algorithm terminates, the relevant auxiliary fields can be projected onto a physical configuration, which is the guaranteed ground state.

The random field is a relevant perturbation at the pure fixed-point, and the random-field fixed-point is at $T = 0$ [7–10]. Hence, the critical behavior is the same everywhere along the phase boundary of Figure 1, and we can predict it simply by staying at $T = 0$ and crossing the phase boundary at $h = h_c$. This is a convenient approach, because we can determine the ground states of the system exactly using efficient optimization algorithms [19,20,24, 43,49–54] through an existing mapping of the ground state to the maximum-flow optimization problem [55]. A clear advantage of this approach is the ability to simulate large system sizes and disorder ensembles in rather moderate computational times. We should underline here that, even

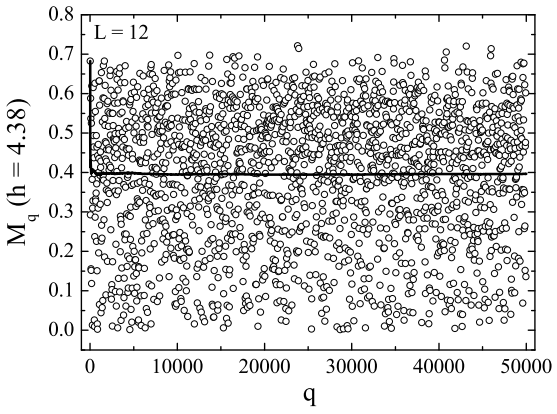

Fig. 2. Disorder distribution of the ground-state order parameter of the $d = 4$ Gaussian RFIM for $L = 12$ and $h = 4.38$ using the *speed mode* representation, i.e., several data points have been removed to make the illustration clearer. The running average over the complete set of samples is shown by the solid line.

the most efficient $T > 0$ Monte Carlo schemes exhibit extremely slow dynamics in the low-temperature phase of these systems and are upper bounded by linear sizes, say for the case of $d = 3$ of the order of $L_{\max} \leq 32$ [48], where L stands for the linear dimension of the lattice. Further advantages of the $T = 0$ approach are the absence of statistical errors and equilibration problems, which, on the contrary, are the two major drawbacks encountered in the $T > 0$ simulation of systems with rough free-energy landscapes [5].

In particular, the application of maximum-flow algorithms to the RFIM is nowadays well established [54]. The most efficient network flow algorithm used to solve the RFIM is the push-relabel algorithm of Tarjan and Goldberg [56]. General proofs and theorems on the push-relabel algorithm can be found in standard textbooks [55]. The version of the algorithm implemented in our study involves a modification proposed by Middleton and co-workers [20, 57,58] that removes the source and sink nodes, reducing memory usage and also clarifying the physical connection [57,58]. The algorithm starts by assigning an excess x_i to each lattice site i, with $x_i = h_i$. Residual capacity variables r_{ij} between neighboring sites are initially set to J. A height variable u_i is then assigned to each node via a global update step. In this global update, the value of u_i at each site in the set $\mathcal{T} = \{j | x_j < 0\}$ of negative excess sites is set to zero. Sites with $x_i \geq 0$ have u_i set to the length of the shortest path, via edges with positive capacity, from i to $\mathcal{T}$.

The ground state is found by successively rearranging the excesses x_i, via *push* operations, and updating the heights, via *relabel* operations. When no more pushes or relabels are possible, a final global update determines the ground state, so that sites which are path connected by bonds with $r_{ij} > 0$ to $\mathcal{T}$ have $\sigma_i = -1$, while those which are disconnected from $\mathcal{T}$ have $\sigma_i = 1$. A push operation moves excess from a site i to a lower height neighbor j, if possible, that is, whenever $x_i > 0$, $r_{ij} > 0$, and $u_j = u_i - 1$. In a push, the working variables are modified according to $x_i \to x_i - \delta$, $x_j \to x_j + \delta$, $r_{ij} \to r_{ij} - \delta$, and $r_{ji} \to r_{ji} + \delta$, with $\delta = \min(x_i, r_{ij})$. Push operations tend to move the positive excess towards sites in $\mathcal{T}$. When $x_i > 0$ and no push is possible, the site is relabelled, with u_i increased to $1 + \min_{\{j | r_{ij} > 0\}} u_j$. In addition, if a set of highest sites $\mathcal{U}$ become isolated, with $u_i > u_j + 1$, for all $i \in \mathcal{U}$ and all $j \notin \mathcal{U}$, the height u_i for all $i \in \mathcal{U}$ is increased to its maximum value, N, as these sites will always be isolated from the negative excess nodes. Periodic global updates are often crucial to the practical speed of the algorithm [57,58]. Following the suggestions of references [20,57,58], we have also applied global updates here every $\mathcal{V}$ relabels, a practice found to be computationally optimum [24,43,25,57, 58].

Using the above described scheme we performed large-scale simulations of the $d = 4$ Gaussian and trimodal RFIM for a wide range of the simulation parameters. In the first part, preliminary runs were executed, including also small systems sizes $\mathcal{V} \leq 6^4$, where $\mathcal{V}$ the total number of spins, in order to probe efficiently the critical h-regime of the model. In the second part, extended simulations have been performed for lattice sizes $L = 6 - 32$ and various disorder strengths in the identified critical regime. For each pair (L, h), the disorder averaging process, denoted hereafter as $[\cdots]_{\rm av}$, has been undertaken by sampling over $Q = 5 \times 10^4$ random-field realizations.

Figure 1 presents evidence of an efficient disorder averaging using as a test platform the Gaussian model. In particular, we plot in this figure the $L = 12$ and $h = 4.38$ disorder distribution of the ground-state absolute value order parameter per spin, defined as $M_{\rm q} = \{|\sum_i \sigma_i| / \mathcal{V}\}_{\rm q}$, where q defines a particular random realization of the external magnetic field h_i and runs over the ensemble of realizations as $q = 1, \cdots, Q$. We have chosen on purpose the random-field value $h = 4.38$, which as will be seen below, is close to the pseudo-critical disorder strength for the lattice size $L = 12$. For these L-dependent pseudo-critical values of h, one expects sample-to-sample fluctuations to be maximized and this becomes clear in Figure 1 through the large deviation of the $M_{\rm q}$ values. In the same panel we also plot the corresponding running average over the data, as illustrated by the solid line. This is a series of averages of different subsets of the full data set, each of which is the average of the corresponding subset of a larger set of data points, over the samples for the simulated ensemble of 5×10^4 independent realizations of the random field.

3 Finite-size scaling analysis

We start the presentation of our numerical data and analysis with panel (a) of Figure 3 for the Gaussian RFIM, where we plot the sample-to-sample fluctuations of the disorder-averaged order parameter $V_{[M]_{\rm av}}$, where $V_{[M]_{\rm av}} = \sqrt{([M^2]_{\rm av} - [M]^2_{\rm av})/(Q-1)}$ and $[M]_{\rm av} = \left[\sum_q M_{\rm q}\right]/Q$, as

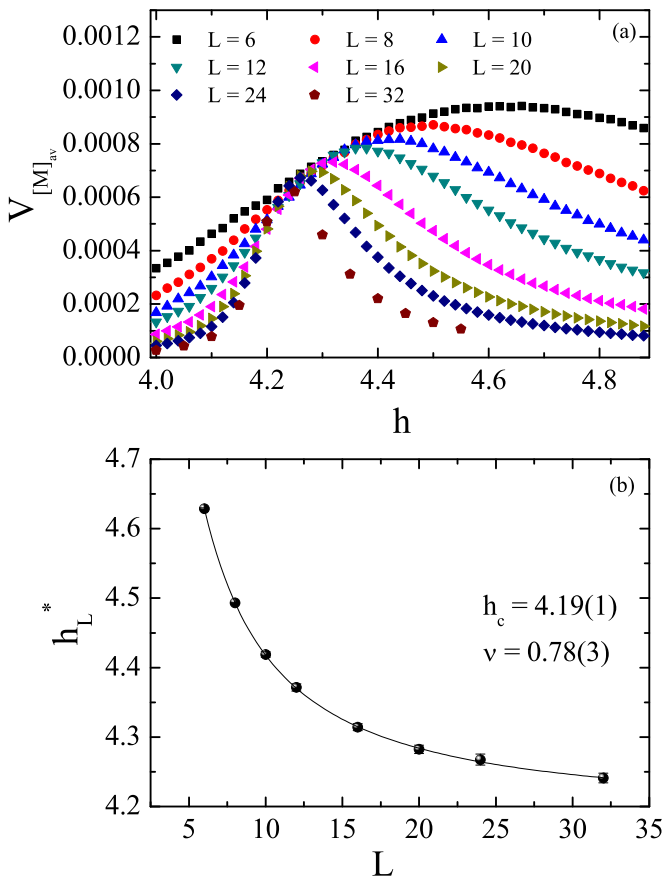

Fig. 3. (color online) (a) Sample-to-sample fluctuations of the order parameter of the $d = 4$ Gaussian RFIM as a function of the disorder strength for various lattice sizes. (b) Finite-size scaling of the pseudo-critical disorder strengths $h^*_{\rm L}$.

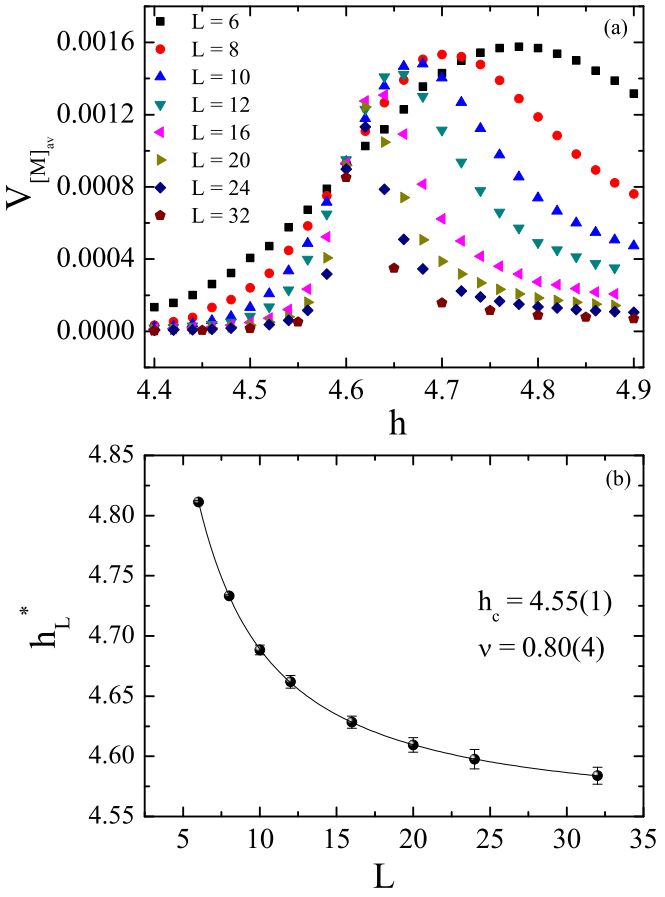

Fig. 4. (color online) Same as in Figure 3 but for the $d = 4$ equal-weight ($p = 1/3$) trimodal RFIM.

a function of the disorder strength h for systems with linear sizes in the regime $L = 6 - 32$. It is clear that for every lattice size L, these fluctuations appear to have a maximum value at a certain value of h, denoted hereafter as $h^*_{\rm L}$, that may be considered in the following as a suitable pseudo-critical disorder strength. By fitting the data points around the maximum first to a Gaussian, and subsequently to a fourth-order polynomial, we have extracted the values of the peak-locations ($h^*_{\rm L}$) by taking the mean value via the two fitting functions, as well as the corresponding error bars. Using now these values for $h^*_{\rm L}$ we consider in panel (b) of the same figure a power-law fitting attempt of the standard shift-like form [59]

$$h^*_L = h_{\rm c} + bL^{-1/\nu}, \qquad (4)$$

that leads to the following estimates for the critical disorder strength and the correlation length exponent: $h_{\rm c} = 4.19(1)$ and $\nu = 0.78(3)$, as also indicated in the figure. These values compare well to previously obtained estimates, also from zero-temperature simulations, namely the values $h_{\rm c} = 4.18(1)$ and $\nu = 0.78(10)$ [46], as well as the values $h_{\rm c} = 4.179(2)$ and $\nu = 0.82(6)$ [47].

Similarly, we present in Figure 4 the corresponding analysis for the equal-weight trimodal RFIM, showing again in panel (a) the sample-to-sample fluctuation of the order parameter and in panel (b) the fitting of the pseudo-critical disorder strengths according to the formula (4). As it can be seen from the fitting results, $h_{\rm c} = 4.55(1)$ and $\nu = 0.80(4)$, the value of the critical exponent of the correlation length agrees within error bars to the estimate of the Gaussian model (see panel (b) of figure 3), verifying the proposed equivalence among the two versions of the models of reference [39]. Moreover, in a more general framework, this result reinforces the strong universality scenario proposed recently for the $d = 3$ RFIM, according to which the universality class of the RFIM is independent of the form of the implemented random-field distribution [25].

Our suggestion of employing the finite-size scaling behavior of the peaks of the sample-to-sample fluctuations of the order parameter was inspired by the intriguing analysis of Efrat and Schwartz [60]. These authors, studying also the $d = 3$ RFIM, showed that the behavior of the sample-to-sample fluctuations in a disordered system may be turned into a useful tool that can provide an independent measure to distinguish between the ordered and disordered phases of the system. The analysis of Figures 3

and 4 above verifies their prediction, and the accuracy in the estimation of relevant phase diagram features consists a clear test in favor of the overall scheme.

Closing we would like to mention that analogous considerations have been undertaken also in the past by various authors for the $d = 3$ RFIM. In particular, Hartmann and Young [51] considered pseudo-critical disorder strengths at the values of h at which a specific-heat-like quantity obtained by numerically differentiating the bond energy with respect to h attains its maximum. On the other hand, Dukovski and Machta [52] identified the pseudo-critical points as those in the $H - h$ plane (with H a uniform external field), where three degenerate ground states of the system show the largest discontinuities in the magnetization. It appears that this method of extracting pseudo-critical points from the maxima of some properly defined thermodynamic quantity is capable of producing very accurate estimates for both the critical disorder strength and the correlation length exponent, assuming that its behavior follows the observed shift behavior of our pseudo-critical disorder strengths $h_{\rm L}^*$. It is well known from the general scaling theory that, even for simple models, the equality between the correlation length exponent and the shift exponent is not a necessary consequence of scaling [61]. Of course, it is a general practice to assume that the correlation length behavior can be deduced by the shift of appropriate thermodynamic functions.

4 Synopsis

We have investigated the ground-state criticality of the four-dimensional random-field Ising model with two types of the field distribution: (i) a Gaussian and (ii) an equal-weight trimodal distribution. In particular, we have estimated for both versions of the model the critical disorder strength $h_{\rm c}$ above which no phase transition takes place and the critical exponent ν of the correlation length. For the Gaussian model (i), the proposed estimates of $h_{\rm c}$ and ν compare well enough to previous estimates in the literature [46,47], verifying the accuracy of the numerical data and scaling scheme. For the version of the model where the random fields have been obtained from an equal-weight trimodal distribution, case (ii), the value of the critical exponent ν supports the original view of Mattis [39] that the two versions of the model share the same universality class. This latter result is also in favor of the strong universality scenario of critical exponents being independent of the field distribution suggested very recently for the three-dimensional random-field Ising model [25]. Note that such a scenario has been questioned throughout the years both at three- and four-dimensions [19,29,30].

Technically, our effort became feasible through the implementation of a modified version of the push-relabel algorithm that enabled us to simulate large system sizes and guaranteed a proper disorder averaging. On physical grounds, we have implemented a scaling approach based on the sample-to-sample fluctuations of the order parameter of the system. The outcome of this analysis indicated that the fluctuations of the system may be used as an alternative successful approach to criticality, as was also recently underlined by Efrat and Schwartz [60].

N.G. Fytas is grateful to Despina Ploussiou for many helpful discussions.

N.G.F. has conceived the work. N.G.F. and P.E.T. have carried out the calculations, analyzed the results, and edited the manuscript.

References

1. Y. Imry, S.-K. Ma, Phys. Rev. Lett. **35**, 1399 (1975)
2. A. Aharony, Y. Imry, S.-K. Ma, Phys. Rev. Lett. **37**, 1364 (1976)
3. G. Parisi, N. Sourlas, Phys. Rev. Lett. **43**, 744 (1979)
4. D.P. Belanger, A.P. Young, J. Magn. Magn. Mater. **100**, 272 (1991)
5. H. Rieger, in *Annual Reviews of Computational Physics II* (ed. D. Stauffer), 295-341, (World Scientific, Singapore 1995)
6. R.L.C. Vink, K. Binder, H. Löwen, Phys. Rev. Lett. **97**, 230603 (2006)
7. J. Villain, Phys. Rev. Lett. **52**, 1543 (1984)
8. A.J. Bray, M.A. Moore, J. Phys. Condens. Matter **18**, L927 (1985)
9. D.S Fisher, Phys. Rev. Lett. **56**, 416 (1986)
10. A.N. Berker, S.R. McKay, Phys. Rev. B **33**, 4712 (1986)
11. J. Bricmont, A. Kupiainen, Phys. Rev. Lett. **59**, 1829 (1987)
12. M.E.J. Newman, B.W. Roberts, G.T. Barkema, J.P. Sethna, Phys. Rev. B **48**, 16533 (1993)
13. J. Machta, M.E.J. Newman, L.B. Chayes, Phys. Rev. E **62**, 8782 (2000)
14. M.E.J. Newman, G.T. Barkema, Phys. Rev. E **53**, 393 (1996)
15. A. Aharony, Phys. Rev. B **18**, 3318 (1978); A. Aharony, Phys. Rev. B **18**, 3328 (1978); D. Andelman, Phys. Rev. B **27**, 3079 (1983)
16. N.G. Fytas, A. Malakis, Eur. Phys. J. B **61**, 111 (2008)
17. S. Galam, J.L. Birman, Phys. Rev. B **28**, 5322 (1983)
18. V.K. Saxena, Phys. Rev. B **30**, 4034 (1984)
19. A.K. Hartmann, U. Nowak, Eur. Phys. J. B **7**, 105 (1999)
20. A.A. Middleton, D.S. Fisher, Phys. Rev. B **65**, 134411 (2002)
21. R.L.C. Vink, T. Fischer, K. Binder, Phys. Rev. E **82**, 051134 (2010)
22. L.A. Fernández, V. Martín-Mayor, D. Yllanes, Phys. Rev. B **84**, 100408(R) (2011)
23. N.G. Fytas, A. Malakis, K. Eftaxias, J. Stat. Mech.: Theory Exp. (2008) P03015
24. P.E. Theodorakis, I. Georgiou, N.G. Fytas, Phys. Rev. E **87**, 032119 (2013)
25. N.G. Fytas, V. Martín-Mayor, Phys. Rev. Lett. **110**, 227201 (2013)
26. B. Ahrens, J. Xiao, A.K. Hartmann, H.G. Katzgraber, Phys. Rev. B **88**, 174408 (2013)
27. H. Rieger, A.P. Young, J. Phys. A: Math. Gen. **26**, 5279 (1993) ; H. Rieger, Phys. Rev. B **52**, 6659 (1995)
28. A. Falicov, A.N. Berker, S.R. McKay, Phys. Rev. B **51**, 8266 (1995)

29. M.R. Swift, A.J. Bray, A. Martian, M. Cieplak, J.R. Banavar, Europhys. Lett. **38**, 273 (1997)
30. J.-C. Anglés d Auriac, N. Sourlas, Europhys. Lett. **39**, 473 (1997); N. Sourlas, Comput. Phys. Commun. **121**, 183 (1999)
31. U. Nowak, K.D. Usadel, J. Esser, Physica A **250**, 1 (1998)
32. P.M. Duxbury, J.H. Meinke, Phys. Rev. E, **64**, 036112 (2001)
33. L. Hernández, H. Ceva, Physica A **387**, 2793 (2008)
34. N. Crokidakis, F.D. Nobre, J. Phys. Condens. Matter **20**, 145211 (2008); O.R. Salmon, N. Crokidakis, F.D. Nobre, J. Phys. Condens. Matter **21**, 056005 (2009)
35. I.A. Hadjiagapiou, Physica A **390**, 2229 (2011); I.A. Hadjiagapiou, Physica A **390**, 3204 (2011); I.A. Hadjiagapiou, Physica A **391**, 3541 (2012)
36. Ü. Akinci, Y. Yüksel, H. Polat, Phys. Rev. E **83**, 061103 (2011)
37. M. Tissier, G. Tarjus, Phys. Rev. Lett. **107**, 041601 (2011)
38. A. Houghton, A. Khurana, F.J. Seco. Phys. Rev. Lett. **55**, 856 (1985)
39. D.C. Mattis, Phys. Rev. Lett. **55**, 3009 (1985)
40. M. Kaufman, P.E. Klunzinger, A. Khurana, Phys. Rev. B **34**, 4766 (1986)
41. R.M. Sebastianes, V. K. Saxena, Phys. Rev. B **35**, 2058 (1987)
42. A.S. de Arruda, W. Figueiredo, R.M. Sebastianes, V.K. Saxena, Phys. Rev. B **39**, 4409 (1989)
43. N.G. Fytas, P.E. Theodorakis, I. Georgiou, Eur. Phys. J. B **85**, 349 (2012)
44. M. Gofman, J. Adler, A. Aharony, A.B. Harris, M. Schwartz, Phys. Rev. Lett. **71**, 1569 (1993); M. Gofman, J. Adler, A. Aharony, A.B. Harris, M. Schwartz, Phys. Rev. B **53**, 6362 (1996)
45. B. Ahrens, A.K. Hartmann, Phys. Rev. B **83**, 014205 (2011)
46. A.K. Hartmann, Phys. Rev. B **65**, 174427 (2002).
47. A.A. Middleton, arXiv:cond-mat/0208182.
48. A.K. Hartmann, H. Rieger, *Optimization Algorithms in Physics*, (Wiley-VCH, Berlin, 2004)
49. Y. Wu, J. Machta, Phys. Rev. Lett. **95** 137208 (2005); Y. Wu, J. Machta, Phys. Rev. B **74**, 064418 (2006)
50. A.T. Ogielski, Phys. Rev. Lett. **57**, 1251 (1986)
51. A.K. Hartmann, A.P. Young, Phys. Rev. B **64**, 214419 (2001)
52. I. Dukovski, J. Machta, Phys. Rev. B **67**, 014413 (2003)
53. E.T. Seppälä, M.J. Alava, Phys. Rev. E **63**, 066109 (2001)
54. M.J. Alava, P.M. Duxbury, C.F. Moukarzel, H. Rieger, in *Phase Transitions and Critical Phenomena*, Vol. 18, edited by C. Domb, J.L. Lebowitz, (Academic Press, San Diego, 2001)
55. C.H. Papadimitriou, *Computational Complexity*, (Addison-Wesley, Reading, MA, 1994)
56. A.V. Goldberg, R.E. Tarjan, J. Assoc. Comput. Mach. **35**, 921 (1988)
57. A.A. Middleton, Phys. Rev. Lett. **88**, 017202 (2002)
58. J.H. Meinke, A.A. Middleton, arXiv:cond-mat/0502471
59. We also tried to iunclude in our fitting ansatz higher-order scaling corrections $(1 + b'L^{-\omega})$, where ω is the well-known correction-to-scaling exponent, however no improvement has been observed in the χ^2/dof quality-control parameter.
60. A. Efrat, M. Schwartz, Physica A **414**, 137 (2014)
61. M.N. Barber, in *Phase Transitions and Critical Phenomena*, edited by C. Domb, J.L. Lebowitz, Vol. 8 (Academic, New York, 1983), p. 146